

Spin-polarized $\nu = 0$ state of graphene: A spin superconductor

Qing-feng Sun^{1,2,*} and X. C. Xie³¹*International Center for Quantum Materials, Peking University, Beijing 100871, China*²*Institute of Physics, Chinese Academy of Sciences, Beijing 100190, China*³*International Center for Quantum Materials and School of Physics, Peking University, Beijing 100871, China*

(Received 14 October 2012; published 24 June 2013)

We study the spin-polarized $\nu = 0$ Landau-level state of graphene. Due to the electron-hole attractive interaction, electrons and holes can bound into pairs. These pairs can then condense into a spin-triplet superfluid ground state: a spin superconductor state. In this state, a gap opens up in the edge bands as well as in the bulk bands, thus it is a charge insulator, but it can carry the spin current without dissipation. These results can well explain the insulating behavior of the spin-polarized $\nu = 0$ state in the recent experiments.

DOI: [10.1103/PhysRevB.87.245427](https://doi.org/10.1103/PhysRevB.87.245427)

PACS number(s): 72.80.Vp, 72.25.-b, 73.43.-f, 74.20.Fg

I. INTRODUCTION

In a magnetic field, monolayer and bilayer graphenes display unconventional Landau-level (LL) spectrum, where the zeroth LL locates the charge neutrality point and has equal electron and hole compositions.¹⁻³ The zeroth LL is fourfold degenerate in monolayer graphene owing to the spin and valley degeneracies, and it is eightfold degenerate in bilayer one due to the additional orbit (or layer) degeneracy. While under a high magnetic field, electron-electron (e-e) interaction can lift the LL degeneracy,²⁻¹³ leading to broken symmetry quantum Hall states and manifesting further integer Hall plateaus outside the normal sequence, which have been experimentally observed.¹⁴⁻²⁸

Recently, the splitting of the zeroth LL has attracted considerable theoretical and experimental interest.⁴⁻³⁴ A bulk gap opening around the energy $E = 0$ is found and a zero Hall conductance plateau at the filling factor $\nu = 0$ has been observed. Both the spin-polarized and valley-polarized $\nu = 0$ states are suggested. At $\nu = 0$, although the Hall conductance shows a plateau, the longitudinal resistance experimentally exhibits an insulating behavior,¹⁴⁻²⁸ which is very different with the zero longitudinal resistance in the conventional quantum Hall effect.

In the valley-polarized $\nu = 0$ state, the valley splitting is larger than the spin splitting and it is a spin singlet state. Now not only $\nu = 0$, but also the spin-up and spin-down filling factors $\nu_{\uparrow} = \nu_{\downarrow} = 0$.³⁴ In this case, the system is without an edge state as shown in Fig. 1(a), so it is insulating for both bulk and edge states, which is consistent with the experiment results.

On the other hand, when the spin splitting is larger than the valley splitting, the system is in the spin-polarized $\nu = 0$ state.^{5,29} Now, however, ν_{\uparrow} and ν_{\downarrow} are not equal to zero although $\nu = \nu_{\uparrow} + \nu_{\downarrow} = 0$. A + valley spin-up (+ \uparrow)LL is occupied by electron and a - valley spin-down (- \downarrow)LL is occupied by hole, leading to a pair of counter-propagating edge states [see Fig. 1(b)] that can carry both spin and charge currents.²⁹⁻³⁴ Some theoretical works have predicted the spin Hall effect in this case.^{32,33} Particularly due to the presence of the edge states, the longitudinal resistance is $(|\nu_{\uparrow}| + |\nu_{\downarrow}|)e^2/h$ and the system should not show an insulating behavior, although a bulk gap exists. However, experimental works have clearly exhibited an insulating behavior, and

the longitudinal resistance increases quickly with decreasing temperature regardless of whether it is a monolayer or bilayer graphene.^{15,18,19,25,26,28} This is very different from the theoretical prediction and seems to indicate the disappearance of the edge states. Some studies mention that the possible reason for this discrepancy is that the counter-propagating edge states are destroyed by disorders.^{25,30,31,33,34} But the sizes of the experimental samples are only a few micrometers, too short to destroy the edge states by localizing the edge electrons. Furthermore, the disorder effect can not explain the strong increase of the longitudinal resistance at low temperature. In short, this discrepancy still lacks a reasonable explanation.

In this paper, the spin-polarized $\nu = 0$ state in graphene under a strong magnetic field is investigated. By considering the unavoidable electron-hole (e-h) attractive interaction, we find that electrons at + \uparrow LL and holes at - \downarrow LL can form spin-triplet e-h pairs. This e-h pair gas can condense at low temperature, leading to the transition to a spin superconductor phase (spin-triplet exciton condensation state)³⁵ associated with the opening of an energy gap for the edge states. Thus, the system exhibits an insulating behavior, consistent with experimental observations.^{15,18,19,25,26,28}

The remainder of this paper is organized as follows. In Sec. II, we introduce the Hamiltonian in the tight-binding representation and derive the formula of the spin-superconductor order parameter. The results are discussed in Sec. III. Finally, the conclusion is presented in Sec. IV.

II. MODEL AND FORMULATION

Let us consider a graphene nanoribbon in a magnetic field. In the tight-binding representation, its Hamiltonian is $\mathcal{H} = \mathcal{H}_0 + \mathcal{H}_I$, where

$$\mathcal{H}_0 = \sum_{\mathbf{i},\sigma} (\epsilon_{\mathbf{i}} - \sigma M) a_{\mathbf{i}\sigma}^{\dagger} a_{\mathbf{i}\sigma} + \sum_{\mathbf{i},\mathbf{i}',\sigma} t_{\mathbf{i}\mathbf{i}'} e^{i\phi_{\mathbf{i}\mathbf{i}'}} a_{\mathbf{i}\sigma}^{\dagger} a_{\mathbf{i}'\sigma} + \text{H.c.},$$

$$\mathcal{H}_I = \sum_{\mathbf{i},\mathbf{i}',\sigma,\sigma' (\mathbf{i}\sigma \neq \mathbf{i}'\sigma')} U_{\mathbf{i}\mathbf{i}'} a_{\mathbf{i}\sigma}^{\dagger} a_{\mathbf{i}\sigma} a_{\mathbf{i}'\sigma'}^{\dagger} a_{\mathbf{i}'\sigma'}$$
(1)

represent the free part and the e-e Coulomb interaction part of the Hamiltonians, respectively. Here $a_{\mathbf{i}\sigma}^{\dagger}$ ($a_{\mathbf{i}\sigma}$) is the electron creation (annihilation) operator at sites \mathbf{i} with spin σ . $\epsilon_{\mathbf{i}}$ is the on-site energy, and M is the spin splitting energy which originates from both the Zeeman effect and the spin

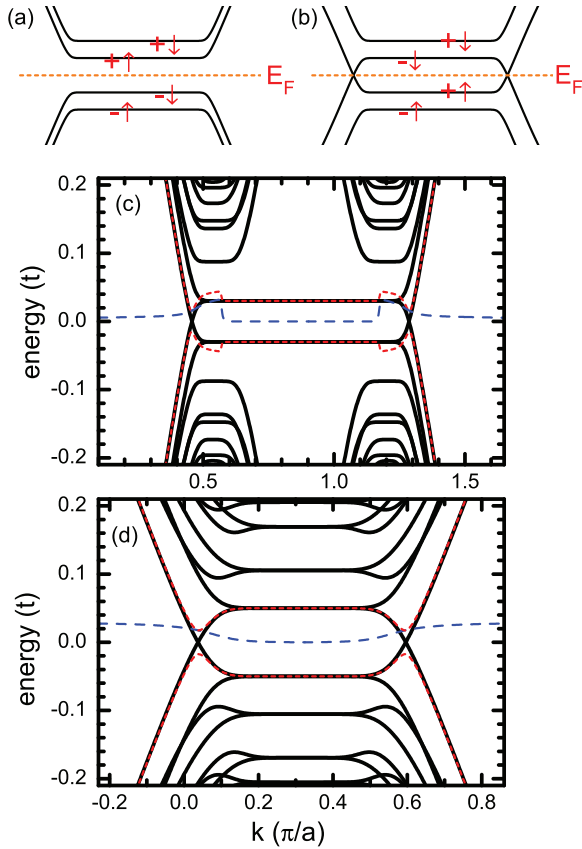


FIG. 1. (Color online) (a) and (b) are the schematic diagrams of the energy spectrum structures for the valley-polarized and spin-polarized $\nu = 0$ states, respectively. (c) and (d) show Δ_k (the blue dashed curves), and the energy spectra for the normal state (the black solid curves) and for the spin superconductor state (the red dotted curves). (c) is for the zigzag edge graphene ribbon with the parameters $N = 200$, $U_c = 15t$, $M = 0.03t$, and $\phi = 0.004$, and (d) is for the armchair edge graphene ribbon with the parameters $N = 282$, $U_c = 25t$, $M = 0.05t$, and $\phi = 0.007$.

polarization induced by the e-e interaction. The second term in \mathcal{H}_0 represents the hopping between the site \mathbf{i} and \mathbf{i}' . Because of the presence of a magnetic field B , a phase $\phi_{\mathbf{i}\mathbf{i}'} = \int_{\mathbf{i}}^{\mathbf{i}'} \mathbf{A} \cdot d\mathbf{l} / \phi_0$ ($\phi_0 = \hbar/e$) is attached in the hopping element $t_{\mathbf{i}\mathbf{i}'}$.³⁶ \mathcal{H}_I is the e-e interaction and $U_{\mathbf{i}\mathbf{i}'}$ is the interaction strength. This Hamiltonian \mathcal{H} can describe both monolayer and bilayer graphene ribbons with arbitrary edge chirality. Considering the ribbon periodicity, the site indices \mathbf{i} can be represented as $\mathbf{i} = (n, j)$ with the slice cell indices n and the atomic indices j in a cell ($j = 1, 2, \dots, N$, and N is the total atom number in a cell). Then the Hamiltonian can be rewritten as

$$\begin{aligned} \mathcal{H}_0 &= \sum_{n,\sigma} \vec{a}_{n\sigma}^\dagger (\mathbf{H}_0 - \sigma M) \vec{a}_{n\sigma} + \sum_{n,\sigma} \vec{a}_{n\sigma}^\dagger \mathbf{H}_1 \vec{a}_{n-1\sigma} + \text{H.c.} \\ \mathcal{H}_I &= \sum_{n,n',\sigma,\sigma'} \vec{n}_{n\sigma}^\dagger \mathbf{U}_{n-n'} \vec{n}_{n'\sigma'}, \end{aligned} \quad (2)$$

where $\vec{a}_{n\sigma} = (a_{n1\sigma}, a_{n2\sigma}, \dots, a_{nN\sigma})^T$ and $\vec{n}_{n\sigma} = (a_{n1\sigma}^\dagger a_{n1\sigma}, a_{n2\sigma}^\dagger a_{n2\sigma}, \dots, a_{nN\sigma}^\dagger a_{nN\sigma})^T$. \mathbf{H}_0 , \mathbf{H}_1 , and $\mathbf{U}_{n-n'}$ are the intracell Hamiltonian, hopping term between two nearest-neighbor cells, and the e-e interaction. By taking the Fourier

transformation $\vec{a}_{n\sigma} = \frac{1}{\sqrt{L}} \sum_k e^{inak} \vec{a}_{k\sigma}$ with the nanoribbon length La and the cell length a , the Hamiltonian \mathcal{H} can be written as $\mathcal{H}_0 = \sum_{k,\sigma} \vec{a}_{k\sigma}^\dagger (\mathbf{H}_k - \sigma M) \vec{a}_{k\sigma}$ with $\mathbf{H}_k = \mathbf{H}_0 + \mathbf{H}_1^\dagger e^{iak} + \mathbf{H}_1 e^{-iak}$, and

$$\mathcal{H}_I = \sum_{\sigma,\sigma',k,k',q} \vec{a}_{k-q\sigma}^\dagger \vec{a}_{k\sigma} \mathbf{U}_{k-k'} \vec{a}_{k'+q\sigma'}^\dagger \vec{a}_{k'\sigma'} \quad (3)$$

with $\mathbf{U}_k = \frac{1}{L} \sum_n e^{inak} \mathbf{U}_n$. In fact, \mathbf{H}_k is the momentum-space Hamiltonian of the free system. Assuming that the eigen-wave functions and eigenvalues of \mathbf{H}_k are $\vec{\Psi}_k^{(j)}$ and $\epsilon_k^{(j)}$: $\mathbf{H}_k \vec{\Psi}_k^{(j)} = \epsilon_k^{(j)} \vec{\Psi}_k^{(j)}$, we have $\mathbf{U}_k^\dagger \mathbf{H}_k \mathbf{U}_k = \epsilon_k$ with $\mathbf{U}_k = (\vec{\Psi}_k^{(1)}, \vec{\Psi}_k^{(2)}, \dots, \vec{\Psi}_k^{(N)})$ and $\epsilon_k = \text{diag}(\epsilon_k^{(1)}, \epsilon_k^{(2)}, \dots, \epsilon_k^{(N)})$. By taking a unitary transformation $\vec{a}_{k\sigma} = \mathbf{U}_k \vec{b}_{k\sigma}$, \mathcal{H}_0 changes into $\mathcal{H}_0 = \sum_{k\sigma} \vec{b}_{k\sigma}^\dagger (\epsilon_k - \sigma M) \vec{b}_{k\sigma}$.

Let us assume that the eigenvalues $\epsilon_k^{(j)}$ have been arranged according of their values from small to large and Fermi level E_F is set at zero. The two nearest bands to E_F are the spin-up $1 + N/2$ -th band and spin-down $N/2$ -th band. Due to the presence of a magnetic field and the spin splitting energy M , the system consists of LLs and is spin-polarized. The spin-up $1 + N/2$ -th (spin-down $N/2$ -th) band is denoted as $+\uparrow$ ($-\downarrow$) LL with its energy $\epsilon_k^{(1+N/2)} - M$ below ($\epsilon_k^{(N/2)} + M$ above) E_F , its carrier being electronlike (holelike), and its band bending upward (downward) as shown in Fig. 1(b). Now the system is at the spin-polarized $\nu = 0$ state, in which a bulk gap $2M$ appears but two edge states cross at E_F . In the following, we focus on these two low-energy bands, and show that the e-e interaction \mathcal{H}_I will create an energy gap for the edge states. Let us introduce the electron and hole annihilation operators: $b_{k\uparrow e} = b_{k\uparrow, 1+N/2}$ and $b_{k\uparrow h} = b_{k\downarrow, N/2}^\dagger$. Then the free Hamiltonian \mathcal{H}_0 reduces to:

$$\mathcal{H}_0 = \sum_k [b_{k\uparrow e}^\dagger (\epsilon_{ke} - M) b_{k\uparrow e} + b_{k\uparrow h}^\dagger (\epsilon_{kh} - M) b_{k\uparrow h}],$$

with $\epsilon_{ke} = \epsilon_k^{(1+N/2)}$ and $\epsilon_{kh} = -\epsilon_k^{(N/2)}$.

As for \mathcal{H}_I , we take the following steps: (i) only the terms whose momenta satisfy $k = k' + q$ in Eq. (3) are kept since the zero momentum e-h pairs are energetically more favorable; (ii) we take the aforementioned unitary transformation and the e-h transformation; (iii) we focus on the two low-energy bands; and (iv) we assume that $U_{\mathbf{i}\mathbf{i}'} = U_c$ while $\mathbf{i} = \mathbf{i}'$ and $U_{\mathbf{i}\mathbf{i}'} = 0$ otherwise, since the on-site e-e interaction is the dominant one. Then the interaction part \mathcal{H}_I reduces to

$$\mathcal{H}_I = - \sum_{k,k'} U_{kk'} b_{k\uparrow e}^\dagger b_{k'\uparrow e}^\dagger b_{k\uparrow h} b_{k'\uparrow h} \quad (4)$$

where

$$U_{kk'} = \frac{1}{L} \sum_j U_{k',jN/2}^* \mathcal{U}_{k,jN/2} U_c \mathcal{U}_{k,j1+N/2}^* \mathcal{U}_{k',j1+N/2}.$$

While at equilibrium, the spin-up electrons (holes) occupy the $+\uparrow$ ($-\downarrow$) LL and its edge state up to the energy $E = E_F = 0$. This is a spin-polarized $\nu = 0$ state that has $U(1)$ symmetry around the σ_z axis. Notice that the interaction \mathcal{H}_I in Eq. (4) between an electron and a hole is attractive. This attractive interaction will not cause the e-h recombination, due to both the spin splitting and the hole band ($-\downarrow$ LL) being above the

electron band ($+\uparrow$ LL).³⁵ However, it can lead to a different instability of the spin-polarized $\nu = 0$ state at low temperature, namely the electrons and holes can form e-h pairs which can then condense to a spin-triplet superfluid state.^{35,37} Notice here the spin splitting (or spin polarization) is a key factor for stable e-h pairs. Under the mean-field approximation, \mathcal{H}_I changes into

$$\mathcal{H}_I = \sum_k [\Delta_k b_{k\uparrow e}^\dagger b_{k\uparrow h}^\dagger + \Delta_k^* b_{k\uparrow h} b_{k\uparrow e}], \quad (5)$$

where $\Delta_k \equiv -\sum_{k'} U_{kk'} \langle b_{k'\uparrow h} b_{k'\uparrow e} \rangle$ is the e-h pair condensation order parameter. So we have the total Hamiltonian $\mathcal{H} = \mathcal{H}_0 + \mathcal{H}_I$:

$$\mathcal{H} = \sum_k (b_{k\uparrow e}^\dagger, b_{k\uparrow h}) \begin{pmatrix} \epsilon_{ke} - M & \Delta_k \\ \Delta_k^* & M - \epsilon_{kh} \end{pmatrix} \begin{pmatrix} b_{k\uparrow e} \\ b_{k\uparrow h} \end{pmatrix}. \quad (6)$$

Now a gap $|\Delta_k|$ opens up in the edge bands [e.g., see Figs. 1(c) and 1(d)], and it needs an energy $2|\Delta_k|$ to break up an e-h pair. So the e-h pair condensed state is more stable than the spin-polarized $\nu = 0$ state, and it is the ground state of the system at low temperature. Since the spins of the electrons and the holes are both up, the e-h pair is spin triplet but charge neutral. The condensed superfluid state is a spin superconductor while it is a charge insulator.^{35,38} It carries spin current dissipationlessly, thus its spin resistance is zero. The spin superconductor also possesses its own unique ‘‘Meissner effect’’.³⁵ Now the system has two possible phases. One is the spin-polarized $\nu = 0$ state (hereafter we named it as normal state for short) at high temperature. It has a bulk gap but two gapless edge bands crossover at the Fermi level, leading to the current flow through the edge states.^{29–34} In the normal phase, the system consists of $U(1)$ symmetry. The other is the spin superconductor state at low temperature, in which both bulk bands and edge bands consist of energy gaps at E_F . Notice that this phase is still a spin polarized one and its filling factor $\nu = 0$ with $\nu_\uparrow = -\nu_\downarrow = 1$. We name it as spin-superconductor spin-polarized $\nu = 0$ state, or spin superconductor state for short. This phase does not contain $U(1)$ symmetry in any direction. In other words, the system breaks $U(1)$ symmetry with the phase transition from the normal phase to the spin superconductor phase.

III. RESULTS AND DISCUSSIONS

From the definition of Δ_k and Hamiltonian (6), we obtain the self-consistent equation of Δ_k : $\Delta_k = -i \sum_{k'} U_{k'k} \int \frac{d\epsilon}{2\pi} f(\epsilon) (\frac{\Delta_{k'}}{A} - \frac{\Delta_k}{A^*})$, where $f(\epsilon)$ is the Fermi distribution function and $A = (\epsilon - \epsilon_{k'e} + M + i0^+) (\epsilon + \epsilon_{k'h} - M + i0^+) - |\Delta_{k'}|^2$. While at zero temperature, the above equation reduces to

$$\Delta_k = \sum_{k'} U_{k'k} \frac{\Delta_{k'}}{\sqrt{(\epsilon_{k'e} + \epsilon_{k'h} - 2M)^2 + 4|\Delta_{k'}|^2}}. \quad (7)$$

From this equation, Δ_k can be self-consistently calculated. In the numerical calculations, we first consider the monolayer zigzag graphene ribbon with the ribbon transverse width $W = (3N/4 - 1)a_0$ and periodic cell length $a = \sqrt{3}a_0$. Here $a_0 = 0.142$ nm is the distance between two nearest-neighbor carbon atoms. We only consider the nearest-neighbor hopping with its

strength $t_{ij} = t = 2.75$ eV, which is set as the energy unit. The on-site e-e interaction $U_c = \frac{e^2}{4\pi\epsilon_0 r} \approx \frac{3.69}{r/a_0} t$ with the distance r between two electrons. $U_c \approx 14.75t$ if $r = a_0/4$.

Fig. 1(c) shows Δ_k and the energy spectrum. For the normal state, although it has a bulk gap due to the spin splitting energy M , two gapless edge states cross at the Fermi level and they can carry both charge and spin currents, causing the sample edge to have a metallic behavior.^{29–34} On the other hand, for the spin superconductor state at low temperature, Fig. 1(c) clearly exhibits a gap opening for the edge bands. Now both edge and bulk bands have the gaps, so it is a charge insulator, consistent with the experimental results.^{14–28} In this state, the spin current can dissipationlessly flow in it, because the condensed e-h pairs with spin 1 can carry the spin supercurrent. Except for the edge states, other parts of the bands are almost the same for both normal and spin superconductor states and their LLs overlap, because the carriers far away from the Fermi level are not energetically favorable to form e-h pairs. Δ_k is large for the edge bands but is vanishingly small for the bulk bands. This means that the condensed e-p pairs mainly distribute near the sample edge, and the spin supercurrent flows along the edges.

Up to now, we only consider the monolayer zigzag edge graphene. In fact, it is similar for graphene with other edge chirality as well as for a bilayer graphene. For example, Fig. 1(d) shows Δ_k and the energy spectrum for the armchair edge graphene nanoribbon with the ribbon width $W = \frac{N-2}{4}\sqrt{3}a_0$ and cell length $a = 3a_0$. The free Hamiltonian exhibits two gapless edge states. The e-h attractive interaction induces a gap in the edge states at low temperature. The order parameter Δ_k is large for the edge bands but is very small for the bulk bands.

Next, we study the zigzag edge graphene nanoribbon in detail. Figures 2(a) and 2(b) show the energy spectrum of the spin superconductor state and Δ_k for different magnetic fields ϕ (here $2\phi = (3\sqrt{3}/2)a_0^2 B/\phi_0$ is the magnetic flux in the honeycomb lattice). For all ϕ , Δ_k exhibits peaks when the original bands cross at E_F and Δ_k is small otherwise. With increasing ϕ , Δ_k increases because a larger magnetic

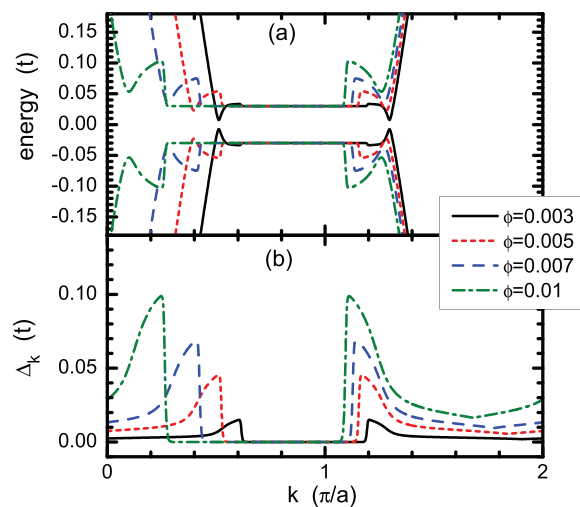


FIG. 2. (Color online) (a) and (b) show the energy spectra of the spin superconductor and the order parameter Δ_k , respectively. The parameters are the same as in Fig. 1(c).

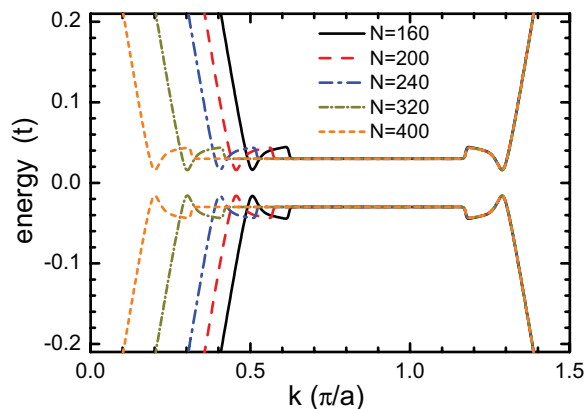


FIG. 3. (Color online) The energy spectra for the spin superconductor state for the different width of nanoribbon. The parameters are the same as in Fig. 1(c).

field leads to a smaller cyclotron radius of carriers, thus a stronger e-h attractive interaction $U_{kk'}$. Particularly, for a large ϕ , the edge-band gap can exceed the bulk-band gap (i.e., $2M$). In this case, the edge states disappear in the whole spin-polarized $\nu = 0$ regime, as has been observed in the experiments.^{15,18,19,25,26,28}

Figure 3 shows the energy spectrum of the spin superconductor state for different widths of nanoribbon. The results show that both the edge-band gap and bulk-band gap are almost independent with the width N , because while under the high magnetic field, the edge states and LLs in the spin-polarized state are independent with the width of nanoribbons.

Let us study the effect of the system parameters on the energy gap. Here the gap is defined as the one of the whole energy spectrum, equal to the smaller one of the bulk and the edge gaps. The gap is independent of the width N of nanoribbon. Figures 4(a), 4(b), and 4(c) show the gap versus the spin splitting energy M , the e-e interaction strength U_c , and the magnetic flux ϕ , respectively. With the increase of M , the gap first increases due to the rising of the bulk gap, and then decreases. As for the gap versus U_c , there exists a threshold U_c^t [see Fig. 4(b)]. While $U_c < U_c^t$, the gap is almost zero, but while $U_c > U_c^t$, the gap increases quickly. When the gap reaches the bulk gap $2M$, it hardly increases further. In this case, although the edge gap can further increase, the gap of the whole energy spectrum is decided by the bulk gap. The results of the gap versus ϕ are similar to those of the gap versus U_c since the increase of ϕ strengthens the effective e-h interaction $U_{kk'}$. In an experiment, normally the spin splitting energy M linearly rises with a magnetic field B . So in Fig. 4(d), we show the gap versus ϕ while $M = 2\mu_B B$ and $4\mu_B B$. The results clearly show that the gap linearly rises and the edge gap is always larger than the bulk gap. Now the edge states disappear in all ϕ value, which is well consistent with the

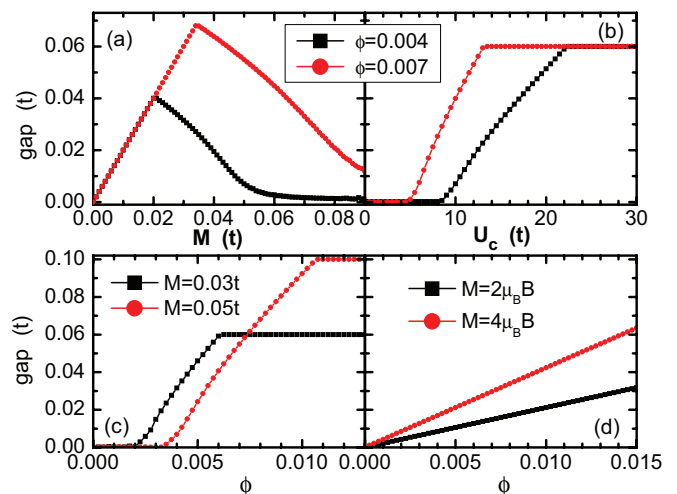


FIG. 4. (Color online) The gap versus M (a), U_c (b), and ϕ (c) and (d). The unmentioned parameters are the same as Fig. 1(c).

experiment results.^{14–28} While $\phi = 0.001$, B is about 25 T, and the gaps are about 3 meV and 6 meV for $M = 2\mu_B B$ and $4\mu_B B$, respectively, to give rise to the corresponding critical temperatures of the phase transition to be about 30 K and 60 K.

Finally, we notice that a recent experiment has simultaneously measured the resistance and the nonlocal resistance in graphene under a magnetic field.¹⁹ They find that the device is an insulator at the neutrality point with $\nu = 0$, but they also see that the nonlocal resistance increases rapidly at low temperature and shows clearly that a spin current is flowing through the device. These findings can be well explained by the presence of a spin superconducting $\nu = 0$ state.

IV. CONCLUSIONS

In summary, the spin-polarized $\nu = 0$ state of graphene under a magnetic field is investigated. We find that it has two phases: one is the normal phase at high temperature and the other is the spin superconductor phase at low temperature. The $U(1)$ symmetry is destroyed under the phase transition from the normal phase to a spin superconductor. For the spin superconductor phase, both edge and bulk bands contain gaps, so it is a charge insulator, but the spin current can flow without dissipation. With the picture of the spin superconductor, many results from recent experiments can be well understood.

ACKNOWLEDGMENTS

This work was financially supported by NBRP of China (2012CB921303, 2009CB929100 and 2012CB821402), NSF-China, under Grant Nos. 11074174, 11121063, 91221302, and 11274364.

*sunqf@iphy.ac.cn

¹A. H. Castro Neto, F. Guinea, N. M. R. Peres, K. S. Novoselov, and A. K. Geim, *Rev. Mod. Phys.* **81**, 109 (2009).

²M. O. Goerbig, *Rev. Mod. Phys.* **83**, 1193 (2011).

³V. N. Kotov, B. Uchoa, V. M. Pereira, F. Guinea, and A. H. Castro Neto, *Rev. Mod. Phys.* **84**, 1067 (2012).

- ⁴E. McCann and V. I. Fal'ko, *Phys. Rev. Lett.* **96**, 086805 (2006).
- ⁵K. Nomura and A. H. MacDonald, *Phys. Rev. Lett.* **96**, 256602 (2006).
- ⁶V. P. Gusynin, V. A. Miransky, S. G. Sharapov, and I. A. Shovkovy, *Phys. Rev. B* **74**, 195429 (2006).
- ⁷M. Ezawa, *J. Phys. Soc. Jpn.* **76**, 094701 (2007).
- ⁸I. A. Luk'yanchuk and A. M. Bratkovsky, *Phys. Rev. Lett.* **100**, 176404 (2008).
- ⁹L. Sheng, D. N. Sheng, F. D. M. Haldane, and L. Balents, *Phys. Rev. Lett.* **99**, 196802 (2007).
- ¹⁰S. Das Sarma and K. Yang, *Solid State Commun.* **149**, 1502 (2009).
- ¹¹J. Jung and A. H. MacDonald, *Phys. Rev. B* **80**, 235417 (2009).
- ¹²E. V. Gorbar, V. P. Gusynin, and V. A. Miransky, *Phys. Rev. B* **81**, 155451 (2010); E. V. Gorbar, V. P. Gusynin, J. Jia, and V. A. Miransky, *ibid.* **84**, 235449 (2011).
- ¹³R. Nandkishore and L. Levitov, *Phys. Rev. Lett.* **104**, 156803 (2010).
- ¹⁴Y. Zhang, Z. Jiang, J. P. Small, M. S. Purewal, Y.-W. Tan, M. Fazlollahi, J. D. Chudow, J. A. Jaszczak, H. L. Stormer, and P. Kim, *Phys. Rev. Lett.* **96**, 136806 (2006).
- ¹⁵Z. Jiang, Y. Zhang, H. L. Stormer, and P. Kim, *Phys. Rev. Lett.* **99**, 106802 (2007).
- ¹⁶J. G. Checkelsky, Lu Li, and N. P. Ong, *Phys. Rev. Lett.* **100**, 206801 (2008).
- ¹⁷J. G. Checkelsky, Lu Li, and N. P. Ong, *Phys. Rev. B* **79**, 115434 (2009).
- ¹⁸A. J. M. Giesbers, L. A. Ponomarenko, K. S. Novoselov, A. K. Geim, M. I. Katsnelson, J. C. Maan, and U. Zeitler, *Phys. Rev. B* **80**, 201403(R) (2009).
- ¹⁹D. A. Abanin, S. V. Morozov, L. A. Ponomarenko, R. V. Gorbachev, A. S. Mayorov, M. I. Katsnelson, K. Watanabe, T. Taniguchi, K. S. Novoselov, and A. K. Geim, *Science* **332**, 328 (2011).
- ²⁰X. Du, I. Skachko, F. Duerr, A. Luican, and E. Y. Andrei, *Nature (London)* **462**, 192 (2009).
- ²¹A. F. Young, C. R. Dean, L. Wang, H. Ren, P. Cadden-Zimansky, K. Watanabe, T. Taniguchi, J. Hone, K. L. Shepard, and P. Kim, *Nat. Phys.* **8**, 550 (2012).
- ²²E. V. Castro, K. S. Novoselov, S. V. Morozov, N. M. R. Peres, J. M. B. Lopes dos Santos, J. Nilsson, F. Guinea, A. K. Geim, and A. H. Castro Neto, *Phys. Rev. Lett.* **99**, 216802 (2007).
- ²³B. E. Feldman, J. Martin, and A. Yacoby, *Nat. Phys.* **5**, 889 (2009).
- ²⁴Y. Zhao, P. Cadden-Zimansky, Z. Jiang, and P. Kim, *Phys. Rev. Lett.* **104**, 066801 (2010).
- ²⁵R. T. Weitz, M. T. Allen, B. E. Feldman, J. Martin, and A. Yacoby, *Science* **330**, 812 (2010).
- ²⁶S. Kim, K. Lee, and E. Tutuc, *Phys. Rev. Lett.* **107**, 016803 (2011).
- ²⁷F. Freitag, J. Trbovic, M. Weiss, and C. Schönenberger, *Phys. Rev. Lett.* **108**, 076602 (2012).
- ²⁸J. Velasco, L. Jing, W. Bao, Y. Lee, P. Kratz, V. Aji, M. Bockrath, C. N. Lau, C. Varma, R. Stillwell, D. Smirnov, F. Zhang, J. Jung, and A. H. MacDonald, *Nat. Nanotechnol.* **7**, 156 (2012).
- ²⁹D. A. Abanin, P. A. Lee, and L. S. Levitov, *Phys. Rev. Lett.* **96**, 176803 (2006).
- ³⁰D. A. Abanin, K. S. Novoselov, U. Zeitler, P. A. Lee, A. K. Geim, and L. S. Levitov, *Phys. Rev. Lett.* **98**, 196806 (2007).
- ³¹E. Shimshoni, H. A. Fertig, and G. V. Pai, *Phys. Rev. Lett.* **102**, 206408 (2009).
- ³²Q.-F. Sun and X. C. Xie, *Phys. Rev. Lett.* **104**, 066805 (2010).
- ³³D. A. Abanin, R. V. Gorbachev, K. S. Novoselov, A. K. Geim, and L. S. Levitov, *Phys. Rev. Lett.* **107**, 096601 (2011).
- ³⁴Y.-T. Zhang, X. C. Xie, and Q.-F. Sun, *Phys. Rev. B* **86**, 035447 (2012).
- ³⁵Q.-F. Sun, Z.-T. Jiang, Y. Yu, and X. C. Xie, *Phys. Rev. B* **84**, 214501 (2011).
- ³⁶W. Long, Q.-F. Sun, and J. Wang, *Phys. Rev. Lett.* **101**, 166806 (2008).
- ³⁷L. N. Cooper, *Phys. Rev.* **104**, 1189 (1956); P. G. de Gennes and P. A. Pincus, *Superconductivity of Metals and Alloys* (Addison-Wesley, Reading, PA, 1989), pp. P93–P95.
- ³⁸H. Liu, H. Jiang, X. C. Xie, and Q.-F. Sun, *Phys. Rev. B* **86**, 085441 (2012).